RSC Advances

This is an *Accepted Manuscript*, which has been through the Royal Society of Chemistry peer review process and has been accepted for publication.

*Accepted Manuscripts* are published online shortly after acceptance, before technical editing, formatting and proof reading. Using this free service, authors can make their results available to the community, in citable form, before we publish the edited article. This *Accepted Manuscript* will be replaced by the edited, formatted and paginated article as soon as this is available.

You can find more information about *Accepted Manuscripts* in the Information for Authors.

Please note that technical editing may introduce minor changes to the text and/or graphics, which may alter content. The journal's standard Terms & Conditions and the Ethical guidelines still apply. In no event shall the Royal Society of Chemistry be held responsible for any errors or omissions in this *Accepted Manuscript* or any consequences arising from the use of any information it contains.

ROYAL SOCIETY OF CHEMISTRY

www.rsc.org/advances

The fish-scale-based porous carbon shows high performance for the removal of methylene blue from aqueous solution.

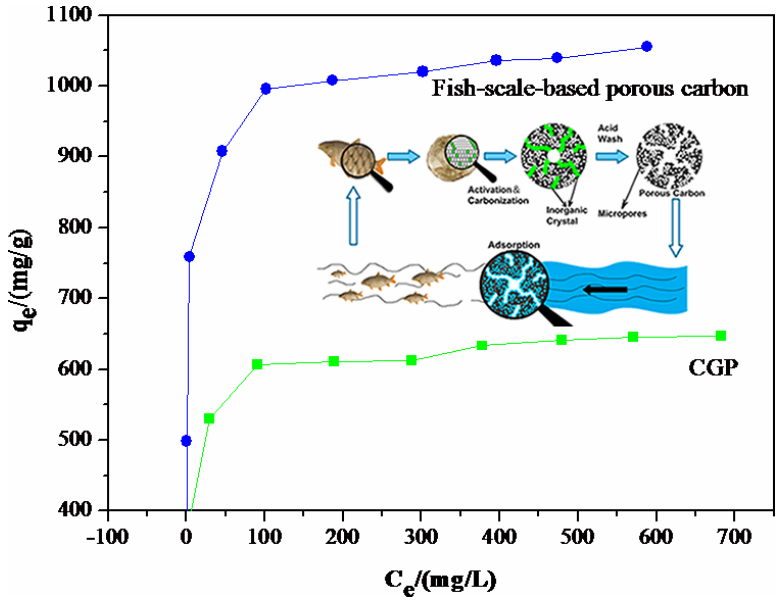


RSC Advances Accepted Manuscript

RSC Advances RSCPublishing

PAPER

# High-performance fish-scale-based porous carbon for the removal of methylene blue from aqueous solution

Zhe Huang,[a] Hongyuan Shao,[a] Bicheng Huang, Chengming Li, Yaqin Huang*, Xiaonong Chen*

*Received (in XXX, XXX) Xth XXXXXXXXX 20XX, Accepted Xth XXXXXXXXX 20XX*
**DOI: 10.1039/b000000x**

**The adsorption of methylene blue (MB) from aquatic systems by the fish-scale-based hierarchical lamellar porous carbon (FHLC) was investigated. In this paper, the FHLC was used as an alternative adsorbent to replace the Norit CGP, a commercial activated carbon, and showed an overall fast and pH-dependent MB adsorption. The effect of contact time, pH and concentration on MB adsorption was investigated. It was found that the adsorption behaviours of FHLC and CGP could be described by a monolayer Langmuir type isotherm. The kinetic data followed the pseudo second-order kinetic model for both activated carbons as the linear correlation coefficients were all above 0.9999. Thermodynamic analyses indicated that the adsorption was an endothermic and spontaneous physisorption process. The maximum Langmuir adsorption capacity of the FHLC was 555.55 mg $g^{-1}$ at pH = 7.07 and 1050.72 mg $g^{-1}$ at pH = 11.00 while that of the CGP was 432.90 mg $g^{-1}$ at pH=7.07 and 649.35 mg $g^{-1}$ at pH=11.00, respectively. The adsorption capacity of the FHLC was much better than that of the CGP at different pH values. Our study shows that fish-scale-based carbon could be used as a high-performance and cost-effective adsorbent to remove MB in aqueous solution in the wastewater treatment.**

## Introduction

The wastewater from the dyeing industry has been one of the major sources for many environmental problems. It contains dyes that are harmful to flora and fauna. In particular, some organic dyes and their products can cause mutagenic or carcinogenic effects on human beings.[1] The presence of even very low concentrations of dyes in the effluent is highly visible and undesirable. The effluent also contains residues of reactive dyes and toxic chemicals. Therefore, wastewater with dye contaminations needs to be properly treated before its release into the environment.[2]

In the complicate procedures of water treatment, activated carbon materials are important due to their significant adsorption ability[3] for the reactive dye, methylene blue (MB), which is widely used for paper coloring, temporary hair colorant, and coating for paper stock, etc, and can be adsorbed onto attapulgite/bentonite[4], peach stone[5], and sodium hydroxide[6]. The MB adsorption capability is one measure to evaluate the property of activated carbon in wastewater treatment,[7] as it reflects the quantity of mesopores on the activated carbon surface.[8] In addition to being used as an adsorbent, activated carbon is also treated as catalysts support [9, 10], energy store[11, 12] in the chemical industry due to their high specific surface, high degree of surface reactivity, and variable surface chemistries. However, as these active carbon materials has high production costs, researchers focus more and more on the development of the alternative and environmental-friendly raw materials for producing cost-effective activated carbon with high adsorption capacity.[3] Most recent studies have concentrated on the agricultural byproducts, such as bamboo[13], coconut shell [14], saw dust [15], cotton stalks[16], fruit stones[17], buffing dust[18].

Fish scales can be a good candidate. It is a byproduct of fisheries, and approximately 50,000 tons of fish scale is discarded as waste every year in China.[19] The main components of fish scales are protein and hydroxyapatite. During the carbonization the protein will provide the carbon source while hydroxyapatite serves as a template to form a specific porous structure. For these reasons, we developed a fish-scale-based porous carbon, which has high surface area and lamellar hierarchical structure.[20] In this article, we used the fish-scale-based hierarchical lamellar porous carbon (FHLC) as an adsorbent to removal the model pollutant, MB, and investigated its adsorption properties. The Scheme 1 shows the representation of the preparation and adsorption for MB onto the FHLC. The influence of pH, the adsorption kinetics, the adsorption capacity and thermodynamics of the FHLC were also studied, and compared with the commercial activated carbon Norit CGP. These results proved the excellent adsorption performance of the FHLC, indicating that it can be a promising adsorbent for treating organic-containing wastewater.

## Materials and methods

### 2.1 Adsorbent preparation and characterization

Raw materials (fish scale) from tilapia were collected from food market. The clean and dry fish scale was precarbonized at 330 °C for 3h in air. The precarbonized powder was mixed with KOH at

RSC Advances Accepted Manuscript

a weight ratio of 1:1, followed by the activation in an $N_2$ atmosphere at 950 °C for 1h. The products were washed with 5 M HCl and hot deionized water until the pH value become neutral, and then heated in a vacuum oven at 120 °C for 24 h to obtain thefish-scale-based carbons.[21] In this article, the fish-scale-based carbon was denoted as FHLC. The commercial activated carbon, CGP Super (Norit), was used as comparison through the whole study.

Textural characterization of the FHLCs was carried out by adsorption/desorption measurement of nitrogen at 77K (ASAP 2020, Micromeritics, USA) and the surface morphologies of FHLCs were examined by scanning electron microscopy (SEM, Model: HITACHI S-4700). The functional groups and elements components of the FHLCs were analyzed by Fourier transform infrared spectroscopy (FT-IR) spectra (Nicolet 6700). The FHLC was examined by zeta potential analysis set (ZetaPALS, Brookhaven Instruments Corporation).

2.2 Methylene blue (MB) solutions preparation

MB ($C_{16}H_{18}ClN_3S{\cdot}3H_2O$, molecular weight 373.90 g $mol^{-1}$) was used as a model pollutant. $Na_2HPO_4$, $NaH_2PO_4$ and 0.01 mol $L^{-1}$ NaOH were used to better control the pH value of MB solutions. All these reagents mentioned were of analytical grade from Sinopharm Chemical Reagent Beijing Co., Ltd. 1000 mg $L^{-1}$ MB solution was prepared and subsequent solutions were all prepared by diluting the stock solution. The diluted solutions were further tested by the UV-2000 at 665 nm to confirm their concentrations.

2.3 Methylene blue adsorption

Adsorption test of MB on different adsorbents were conducted in a batch process by mixing 0.005g adsorbent with 5 mL/10 mL different concentrations of MB solutions in a sealed container. All containers were placed in water bath (30±0.5) °C with the constant temperature to reach the equilibrium. The containers were then removed and the final concentrations of the dye in the solutions were analyzed. The solutions were diluted to a proper concentration as required so that their absorbance remained with the linear calibration range. The upper solution with the less activated carbon partial was test by UV-2000 at 665 nm. Another container with the same MB solution without adsorbent was also processed as a blank team. Measurements on all samples were repeated twice. To better understand the effects of pH value, two pH values of 7.07 and 11.00 were selected in the experiments.

The amount of adsorption at equilibrium ($q_e$/mg $g^{-1}$) was calculated by qe = ($C_0$-$C_e$) V/m, where $C_0$ and $C_e$ (mg $L^{-1}$) are MB solutions concentration at initial and equilibrium, respectively. V is the volume of the solutions (L), while m is the mass of the adsorbent used (g). Similarly, the amount of adsorption at time t ($q_t$/ mg $g^{-1}$) was calculated using $q_t$ = ($C_0$-$C_e$) V/m.

## Results and discussion

3.1 Characterization of adsorbent

Figure 1 showed the surface morphologies of the FHLC and MB adsorbed FHLC (FHLC-MB). It could be seen that the FHLC (Fig. 1(a)) had the lamellar structure and pores on the surface. The large-size pores were analogous to channels surrounded by the small size pores. This structure had high specific surface area and large pore volume. After the MB absorption on the FHLC, most small size pores were filled and parts of large size pores were filled, showing less developed pore structure compared to the FHLC (Fig. 1(b)). These findings were consistent with our assumptions (Scheme 1).

The stronger adsorption ability of the FHLC was further supported by the textural characterization. The BET surface and pore volume of the FHLC was 2273 $m^2$ $g^{-1}$ and 2.74 $cm^3$ $g^{-1}$, respectively, with an average pore diameter of 4.47 nm. These parameters were much higher than those of the CGP (Table 1). Owing to the high specific surface area, large pore volume and ideal porous structure, the FHLC was promising as the adsorbent for wastewater treatment. So we focus on the discussion of the adsorption behavior and kinetics for M B onto the FHLC in the following.

The FT-IR spectrum of FHLC (Fig. 2) showed the characteristic peaks of the stretching vibration of O-H, C=C, C=O, COOH, and C–O respectively at 3429 $cm^{-1}$, 2363 $cm^{-1}$, 1620 $cm^{-1}$, 1440 $cm^{-1}$, 1112 $cm^{-1}$, respectively. It indicated that the FHLC has an abundance of functional groups, which are beneficial for the adsorption process. After the MB adsorption, most of these characteristic peaks of FHLC-MB remain the same as those of FHLC, except the COOH peak. This could be attributed to the neutralization reaction during the pH controlling process, suggestin that the process of MB adsorption on the FHLC was mainly a physical adsorption.

3.2 Effect of contact time

Since adsorption isotherms are related to the equilibrium conditions, we measured the contact time for each adsorption system to reach its equilibrium condition. The effects of contact time in the range 1-24 h were studied using different concentration of MB solution, pH = 7.07 and 11.00 at the temperature of (30±0.5) °C. The adsorption percentage, which was defined as the adsorption quantity over the maximum adsorption quanity, increased with the increased contact time and MB concentration. This agreed with Pavan's conclusion.[22] The adsorption percentage of the FHLC was much higher than that of CGP when there were a few minutes before reaching unity (Fig. 3(a)). However, it took more time to reach the adsorption equilibrium for FHLC when the concentration was closed to or exceed to the maximum adsorption amount. After 24 h, no detectable changes could be observed for all samples at different pH values. As a consequence, subsequent adsorption experiments were all performed for 24 h, a period which was assumed to be enough for performing all the adsorption processes.

3.3 Adsorption isotherms

The adsorption isotherms are fundamental to reveal the process of adsorption molecules that distribute between the liquid phase and the solid phase when the system reaches its equilibrium at a fixed temperature. Once a suitable model can be found to fit the isotherm data, it can serve the design purpose. In general, Langmuir and Freundlich isotherms are enough for evaluation. Thus we applied them in this experiment.

3.3.1 Langmuir isotherm

The Langmuir isotherm is represented by the following equation

RSC Advances Accepted Manuscript

 This journal is © The Royal Society of Chemistry [2014]

(1):

$$C_e/q_e=1/q_mK_L+Ce/q_m \quad (1)$$

Where $C_e$ is the equilibrium concentration of the MB solution (mg $L^{-1}$), $q_e$ is the amount of adsorbate adsorbed per unit mass of adsorbate (mg $g^{-1}$), and $q_m$ and $K_L$ are Langmuir constants which related to the adsorption capacity and rate of adsorption, respectively. The data were analyzed using the Langmuir equation and the results are shown in Table 2. The linear plot of $C_e/q_e$ versus $C_e$ shows that adsorption follows the Langmuir isotherm. Values of $q_m$ and $K_L$ can be calculated from the slope and the intercept of the linear plot.

As seen from Fig. 3(b), equilibrium uptake increased with the increase of the pH value in the range of experimental concentration and the maximum adsorption capacity of FHLC stays higher than that of CGP at both of pH values. Due to the FHLC's porous structure, the maximum monolayer adsorption capacity increased from 555.55 mg $g^{-1}$ at pH = 7.07 to 1050.72 mg $g^{-1}$ at pH=11.00 while the CGPs were 432.90 mg $g^{-1}$ at pH = 7.07 and 649.35 mg $g^{-1}$ pH = 11.00, respectively. The pH at point zero charge of the FHLC tested by the ZetaPALS is about 4.6. Therefore, there would be more and more negatively charged sites in the surface of FHLC when the pH value increases from 7 to 11. Methylene blue, a highly charged molecule (pKa less than or equal to 1), [22] when in neutral and alkaline conditions, it mainly exists as cationic MB. The electrostatic attraction between the cationic MB and FHLC is benefit for the removal of MB from dye water. Besides, lower adsorption at neutral pH was probably due to the presence of excess of $H^+$ ions competing with the dye cations for adsorption sites. [23] The Langmuir isotherms of the FHLC and Norit CGP at different temperature and different values of pH are also showed in Fig. 3(b).

Dimensionless equilibrium parameter ($R_L$) is another essential characteristic of the Langmuir isotherm, as defined:

$$R_L=1/(1+[K_L\times C_0]) \quad (2)$$

The value of $R_L$ indicates the type of the isotherm to be unfavorable ($R_L > 1$), linear ($R_L = 1$), favorable ($0 < R_L < 1$) or irreversible ($R_L = 0$). Values were found to be 0.0087 and 0.0096 for the FHLC and the CGP at pH =7.07, respectively. However, at pH = 11.00, the RL value were 0.00041 and 0.0063 for the FHLC and the CGP, respectively. The results indicate that the carbon samples are favored for the MB adsorption under conditions used in this study.

3.3.2 Freundlich isotherm

The Freundlich isotherm model is expressed by the following equation (3):

$$\log q_e=\log K_F+1/n \log C_e \quad (3)$$

Where $K_F$ and n are Freundlich constants, $K_F$ (mg $g^{-1}(mg^{-1})^{1/n}$) is the adsorption capacity of the adsorbent that is defined as the adsorption or distribution coefficient and represents the quantity of the MB solution onto the activated carbon adsorbent for a unit equilibrium concentration, while n reveals how favorable the adsorption process is. The plot of $\log q_e$ versus $\log C_e$ with slope 1/n ranging between 0 and 1 is a measure of adsorption intensity or surface heterogeneity. The adsorbent surface becomes more heterogeneous as the value of 1/n gets closer to 0.[23]

In Table 2, the 1/n slopes for all the samples at different pH values are close to 0, while the $K_F$ value and linear correlation coefficient increased for both samples as the pH value increased. The $R^2$ calculated from Freundlich isotherm equation is closer to 1, indicating that the adsorption processes also follows the Freundlich isotherm. Compared to FHLC, the slope value decreased while the CGP increased as the pH value increased from 7.07 to 11.00, which means that FHLC became more heterogeneous as the pH value is increased. However the values of $R^2$ values obtained from Freundlich isotherm equation were lower than that from Langmuir isotherm equation. Furthermore, the experimental adsorption capacity ($q_e$) were close to those of theoretical adsorption capacity ($q_m$) calculated from Langmuir isotherm equation. This suggests that Langmuir isotherm model could better describe the adsorption equilibrium process. This also indicates the monolayer coverage of MB on the composite adsorbents.

3.4 Adsorption kinetics

Adsorption kinetics is one of the main characteristics to define the adsorption efficiency and to explain the adsorption mechanism. In order to investigate the adsorption processes of MB dyes on the FHLC and CGP, kinetic analysis were conducted using pseudo-first and second-order models.

3.4.1 The first-order kinetic model

The rate constant of adsorption is determined from the first- order rate expression given by Lagergren and Svenska as below:

$$\ln(q_e-q_t)=\ln q_e-k_1t \quad (4)$$

Where $q_e$ and $q_t$ are the amounts of MB adsorbed (mg $g^{-1}$) at equilibrium and at time t (h), respectively, and $k_1$ ($min^{-1}$)is the rate constant of adsorption ($h^{-1}$). As shown in Table 5, $k_1$ values which are shown in Table 5 were calculated from the plots of $\ln(q_e - q_t)$ versus t at a specific starting concentration of MB solution. Here the MB starting concentrations were set to be slightly more than the maximum adsorption for all samples at different pH values.

At pH = 7.07, both the FHLC and CGP cannot be fit for the first-order kinetic model as the $R^2$ values were only 0.6356 and 0.8954, respectively. And the adsorption process also cannot be better fit using the first-order kinetic model at pH = 11.00 as the $R^2$ values were 0.8974 and 0.9736 for the FHLC and CGP

3.4.2 The second-order kinetic model

The second-order kinetic model is expressed as below:

$$t/q_t=1/(k_2q_e^2)+t/q_e \quad (5)$$

Where $k_2$ [g (mg h)$^{-1}$] is the rate constant of second-order adsorption and the values of $k_2$ were calculated from the plots of $t/q_t$ versus t.

It is clear to see that both FHLC and CGP can be better fit by the second-order kinetic model at different pH values as the linear correlation coefficients were all above 0.9999.

3.5 Thermodynamic analyses

To estimate the temperature effect on the adsorption of MB onto FHLC and CGP, the free energy change ($\Delta G_0$), enthalpy change ($\Delta H_0$), and entropy change ($\Delta S_0$) were determined. The Langmuir isotherm was used to calculate thermodynamic parameters using the following equations:

$$\Delta G_0= -RT\ln(K_L) \quad (6)$$

$$\ln(K_L)=\Delta S_0/R-\Delta H_0/RT \quad (7)$$

Where $K_L$ is the Langmuir equilibrium constant (L/g); R is the

RSC Advances Accepted Manuscript

gas constant (8.314 J/mol $K^{-1}$) and T is the temperature (K). Considering the relationship between $\Delta G_0$ and $K_L$, $\Delta H_0$ and $\Delta S_0$ were determined from the slope and intercept of the van't Hoff plots of $\ln(K_L)$ versus 1/T. Table 6 presents the thermodynamic parameters at various temperatures. The negative values confirm the feasibility of the process and the spontaneous nature of the adsorption.

In general, $\Delta H_0$ value less than 40kJ/mol indicates that the adsorption process is physisorption.[24] The positive value of $\Delta S^0$ demonstrates the increased randomness at the solid–solute interface and the affinity of the FHLC for the MB, This is a direct consequence of enhancement of the mobility and extent of penetration within the activated carbon pores and overcoming the activation energy barrier and enhancing the rate of intra-particle diffusion as well. The values of $\Delta G_0$ suggest the adsorption is a spontaneous process and adsorption rate improves when the temperature's increased. The positive value of $\Delta H_0$ indicates that the adsorption reaction is endothermic.

## Conclusion

In summary, the high performance of fish-scale-based porous carbon for the removal of methylene blue from the aqueous solution has been demonstrated. Their adsorption capacity was shown to be better than that of CGP for dye adsorption at different pH values. The maximum adsorption capacity of the FHLC was 555.55 mg $g^{-1}$ at pH = 7.07 and 1050.72 mg $g^{-1}$ at pH = 11.00, while capacity for the CGP was 432.90 mg g-1 and 649.35 mg $g^{-1}$ at pH = 7.07 and 11.00, respectively. Although both of the two carbons were prone to alkaline condition for MB adsorption, the FHLC would be a faster separation adsorbent to remove MB from the wastewater. Adsorption behaviors of the FHLC were described by a monolayer Langmuir type isotherm while kinetic data obey the pseudo second-order kinetic model for MB. Thermodynamic analyses indicated that the adsorption for MB direct dyes onto the FHLC and CGP was endothermic and spontaneous, and via a physisorption process. Considered the adsorption performance of the FHLC, the fish-scale-based activated carbon is a promising adsorbent in the water treatment.

### Acknowledgement

Financial support from the National Science Foundation of China (No. 51272017) is gratefully appreciated.

## Notes and references

*State Key Laboratory of Chemical Resource Engineering, The Key Laboratory of Beijing City on Preparation and Processing of Novel Polymer Materials, Beijing University of Chemical Technology, 15 BeiSanhuan East Road, Beijing, 100029, P.R. China.*

** E-mail: huangyq@mail.buct.edu.cn, Fax: +86 10 6443 8266, Tel: +86 10 6443 8266; chenxn@mail.buct.edu.cn, Fax:+86 10 6443 8266, Tel: +86 10 6443 8266*

*[&]These authors contributed equally to this work and should be considered as co-first authors*

1 Liu, T., Li, Y., Du, Q., Sun, J., Jiao, Y., Yang& Wu, D.. Adsorption of methylene blue from aqueous solution by graphene. *Colloids and Surfaces B: Biointerfaces*, 2012, **90**, 197-203.

2 Sun, L., Wan, S., & Luo, W.. Biochars prepared from anaerobic digestion residue, palm bark, and eucalyptus for adsorption of cationic methylene blue dye: Characterization, equilibrium, and kinetic studies. *Bioresource technology*, 2013, **140,** 406-413

3 Dias, J.M., Alvim-Ferraz, M.C.M., Almeida, M.F., Rivera-Utrilla, J., Sánchez-Polo, M.. Waste materials for activated carbon preparation and its use in aqueous-phase treatment: *A review. Journal of Environmental Management*, 2007, **85**, 833-846.

4 Liu, Y., Kang, Y., Mu, B., & Wang, A.. Attapulgite/bentonite interactions for methylene blue adsorption characteristics from aqueous solution. *Chemical Engineering Journa*l, 2014, **237**, 403-410.

5 Duranoğlu, D., Trochimczuk, A. W., & Beker, Ü.. A comparison study of peach stone and acrylonitrile-divinylbenzene copolymer based activated carbons as chromium (VI) sorbents. *Chemical Engineering Journal*, 2010,**165**(1), 56-63.

6 Zhang, J., Ping, Q., Niu, M., Shi, H., & Li, N.. Kinetics and equilibrium studies from the methylene blue adsorption on diatomite treated with sodium hydroxide. *Applied Clay Science*, 2013, **83**, 12-16.

7 Bestani, B., Benderdouche, N., Benstaali, B., Belhakem, M., Addou, A.. Methylene blue and iodine adsorption onto an activated desert plant. *Bioresource Technology*, 2008, **99**, 8441-8444.

8 Vitidsant, T., Suravattanasakul, T., Damronglerd, S.. Production of activated carbon from palm-oil shell by pyrolysis and steam activation in a fixed bed reactor. ScienceAsia, 1999, **25**, 211-222.

9 Guillén, E., Rico, R., López-Romero, J.M., Bedia, J., Rosas, J.M., Rodríguez-Mirasol, J., Cordero, T.. Pd-activat*ed carbon catalysts* for hyd**rog**enation and Suzuki reactions. *Applied Catalysis A-General*, 2009, **368**, 113-120.

10 Maia, F., Silva, R., Jarrais, B., Silva, A.R., Freire, C., Pereira, M.F.R., Figueiredo, J.L.. Pore tuned *activated carbons as supports for an enantios*elective **m**olecular catalyst. *Journal of Colloid and Interface Science*, 2008, **328**, 314-323.

11 Liu, B., Shioyama, H., Akita, T., Xu, Q.. Metal-Organic Framework as a Template for Porous Carbon Synthesis. *Journal of the American Chemical Society*, 2009, **130**, 5390-5391.

12 Xia, K.S., Gao, Q.M., Jiang, J.H., Hu, J.. Hierarchical porous carbons with controlled micropores and mesopores for supercapacitor electrode materials. *Carbon*, 2008, **46**, 1718-1726.

13 Hameed, B.H., Din, A.T.M., Ahmad, A.L.. Adsorption of methylene blue onto bamboo-based activated carbon: Kinetics and equilibrium studies. *Journal of Hazardous Materials*,2007, **141**, 819-825.

14 Afrane, G., Achaw, O.W.. Effect of the concentration of inherent mineral elements on the adsorption capacity of coconut shell-based activated carbons. *Bioresource Technology*, 2008, **99**, 6678-6682.

15 Prakash-Kumar, B.G., Shivakamy, K., Miranda, L.R., Velan, M.. Preparation of steam activated carbon from rubberwood sawdust (Hevea brasiliensis) and its adsorption kinetics. *Journal of Hazardous Materials*, 2006, **B136**, 922-929.

16 Li, K.Q., Zheng, Z., Huang, X.F., Zhao, G.H., Feng, J.W., Zhang, J.B.. Equilibrium, kinetic and thermodynamic studies on the adsorption of 2-nitroaniline onto activated carbon prepared from cotton stalk fibre. *Journal of Hazardous Materials*, 2009, **166**, 213-220.

17 Aygűn, A., Yenisoy-Karakaş, S., Duman, I.. Production of granular activated carbon from fruit stones and nutshells and evaluation of their physical, chemical and adsorption properties. *Microporous and Mesoporous Materials*, 2003, **66**, 189-195.

18 Sekaran, G., Shanmugasundaram, K.A., Mariappan, M.. Characterization and utilisation of buffing dust generated by the leather industry. *Journal of Hazardous Materials*, 1998, **B63**, 53-68.

19 Cao, J.. Research progress and application prospect of Fish scale collagen. *Fisheries Science & Technology Information,* 2009, **36**, 41-43.

20 Weixin Chen, Hao Zhang, Yaqin Huang and Weikun Wang. A fish scale based hierarchical lamellar porous carbon material obtained using a natural template for high performance electrochemical capacitors. *Journal of Materials Chemistry*, 2010, **20**, 4773-4775

21 Xu, B., Chen, Y.F., Wei, G., Cao, G.P., Zhang, H., Yang, Y.S.. Activated carbon with high capacitance prepared by NaOH

RSC Advances Accepted Manuscript

 This journal is © The Royal Society of Chemistry [2014]

activation for supercapacitors. *Materials Chemistry and Physics*, 2010, **124,** 504-509.

22 Ziv G, Heavner J E. Permeability of the blood‐milk barrier to methylene blue in cows and goats[J]. Journal of veterinary pharmacology and therapeutics, 1984, 7(1): 55-59.

23 Yao, Y., Xu, F., Chen, M., Xu, Z., & Zhu, Z.. Adsorption behavior of methylene blue on carbon nanotubes. *Bioresource technology*, 2010, **101**(9), 3040-3046.

24 Kara, M., Yuzer, H., Sabah, E., Celik, M.S.. Adsorption of cobalt from aqueous solutions onto sepiolite. *Water Research*, 2013, **37**, 224–232.

25 Shaochen Wei, Dongtian Li, Zhe Huang, Yaqin Huang, Feng Wang. High-capacity adsorption of Cr(VI) from aqueous solution using a hierarchical porous carbon obtained from pig bone. *Bioresource Technology*, 2013, **134**,407-411.

RSC Advances Accepted Manuscript

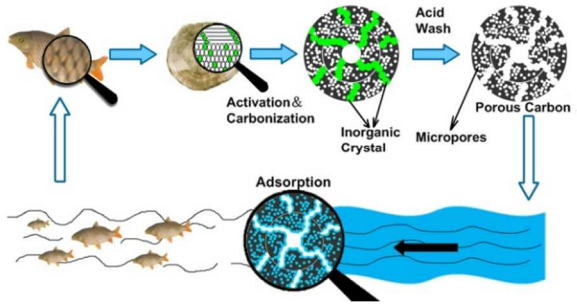


**Scheme 1** Scheme of the preparation and adsorption for MB onto the FHLC from aqueous solution

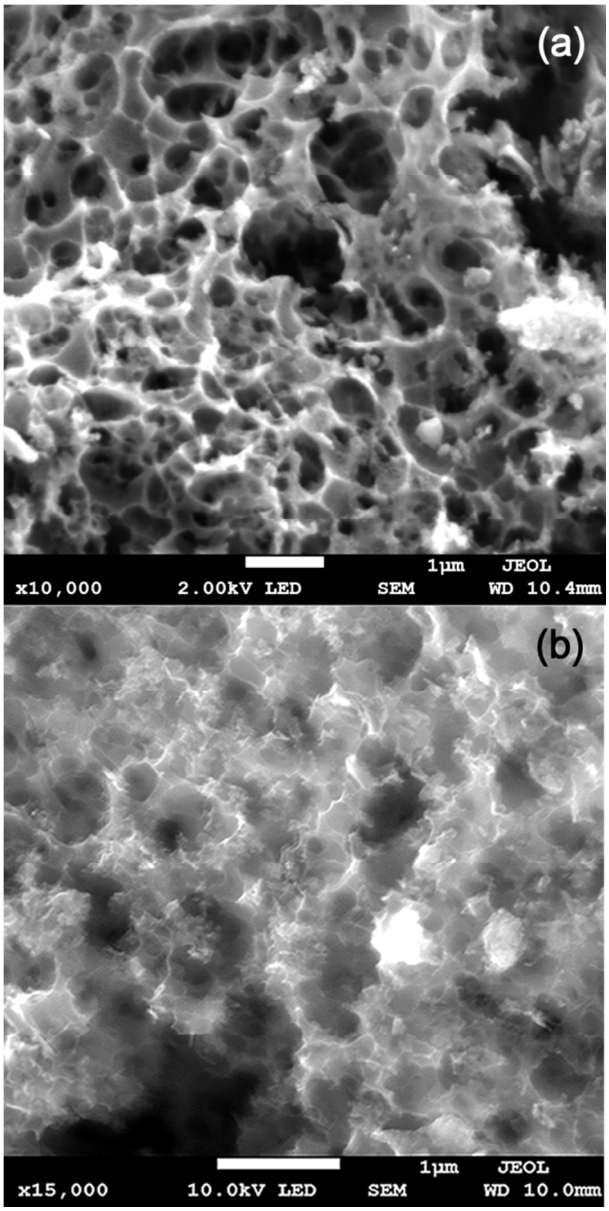


**Fig. 1** The surface morphologies of the FHLC and the FHLC-MB

**Table1** Textural characteristics of the FHLC and CGP.[20,25]

| Sample | FHLC | CGP |
|---|---|---|
| Specific surface area ($m^2$ $g^{-1}$) | 2273 | 1281 |
| Pore volume ($cm^3$ $g^{-1}$) | 2.74 | 1.13 |
| Average pore diameter (nm) | 4.47 | 3.14 |

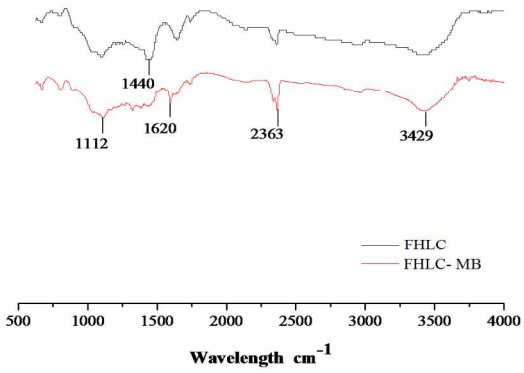


**Fig. 2** The FT-IR spectrum of the FHLC and FHLC-MB

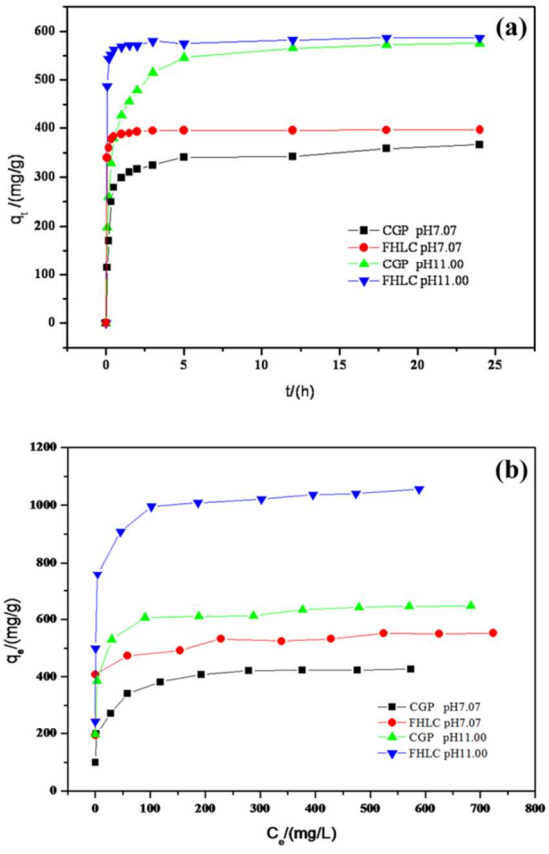


**Fig. 3** (a) The relationship between adsorption quantity and time onto the FHLC and CGP for MB at 30℃(The initial concentration is 200mg/L and 300mg/L) and (b) adsorption isotherm for MB onto FHLC and CGP for pH=7.07and 11.00 at 30℃

RSC Advances Accepted Manuscript


This journal is © The Royal Society of Chemistry [2014]

**Table 2** Langmuir and Freundlich isotherm constant for MB at 30 °C

| Sample | pH | Langmuir isotherm | | | | | Freundlich isotherm | |
|---|---|---|---|---|---|---|---|---|
| | | $q_m$ (mg $g^{-1}$) | $K_L$ ($Lmg^{-1}$) | $R^2$ | $R_L$ | 1/$n$ | $K_F$[(mg $g^{-1}$)($mg^{-1}$)$^{1/n}$] | $R^2$ |
| FHLC | 7.07 | 555.55 | 0.1137 | 0.9991 | 8.7E-03 | 0.0641 | 566.98 | 0.9176 |
| CGP | 7.07 | 432.9 | 0.1031 | 0.9993 | 9.6E-03 | 0.1783 | 520.98 | 0.9613 |
| FHLC | 11.00 | 1050.72 | 0.2452 | 0.9997 | 4.1E-03 | 0.0972 | 1164.98 | 0.9272 |
| CGP | 11.00 | 649.35 | 0.1554 | 0.9996 | 6.3E-03 | 0.0909 | 695.52 | 0.9321 |

**Table 3** Langmuir and Freundlich isotherm constant for MB at 40 °C

| Sample | pH | Langmuir isotherm | | | | | Freundlich isotherm | |
|---|---|---|---|---|---|---|---|---|
| | | $q_m$ (mg $g^{-1}$) | $K_L$ (L $mg^{-1}$) | $R^2$ | $R_L$ | 1/$n$ | $K_F$[(mg $g^{-1}$)($mg^{-1}$)$^{1/n}$] | $R^2$ |
| FHLC | 7.07 | 671.14 | 0.1249 | 0.9992 | 7.9E-03 | 0.0834 | 705.73 | 0.9373 |
| CGP | 7.07 | 510.2 | 0.1161 | 0.9987 | 8.5E-03 | 0.1611 | 606.99 | 0.9801 |
| FHLC | 11.00 | 1117.84 | 0.2831 | 0.9994 | 3.5E-03 | 0.0962 | 1250.75 | 0.9329 |
| CGP | 11.00 | 775.19 | 0.1802 | 0.9993 | 5.5E-03 | 0.0923 | 837.70 | 0.8901 |

**Table 4** Langmuir and Freundlich isotherm constant for MB at 50 °C

| Sample | pH | Langmuir isotherm | | | | | Freundlich isotherm | |
|---|---|---|---|---|---|---|---|---|
| | | $q_m$ (mg $g^{-1}$) | $K_L$ (L $mg^{-1}$) | $R^2$ | $R_L$ | 1/$n$ | $K_F$[(mg $g^{-1}$)($mg^{-1}$)$^{1/n}$] | $R^2$ |
| FHLC | 7.07 | 787.4 | 0.1402 | 0.9995 | 7.1E-03 | 0.1128 | 861.69 | 0.8750 |
| CGP | 7.07 | 591.72 | 0.1241 | 0.9984 | 8.0E-03 | 0.1807 | 741.60 | 0.9776 |
| FHLC | 11.00 | 1283.91 | 0.3054 | 0.9994 | 3.3E-03 | 0.0637 | 1362.07 | 0.9005 |
| CGP | 11.00 | 840.34 | 0.2088 | 0.9993 | 4.8E-03 | 0.0780 | 898.75 | 0.8722 |

**Table 5** First-order kinetic and Second-order kinetic constant for MB at 30 °C

| Sample | pH | First-order kinetic model | | Second-order kinetic model | |
|---|---|---|---|---|---|
| | | $k_1$($h^{-1}$) | $R^2$ | $k_2$[g(mg h)$^{-1}$] | $R^2$ |
| FHLC | 7.07 | 0.1194 | 0.6356 | 0.128 | 0.9997 |
| CGP | 7.07 | 0.0895 | 0.7779 | 0.010 | 0.9999 |
| FHLC | 11.00 | 0.1541 | 0.8974 | 0.042 | 0.9999 |
| CGP | 11.00 | 0.1684 | 0.9736 | 0.006 | 0.9999 |

**Table 6** Thermodynamic parameters for MB adsorbed by the FHLC and CGP

| Sample | pH | -$\Delta G^0$(kJ/mol) | | | $\Delta H^0$ | $\Delta S^0$ |
|---|---|---|---|---|---|---|
| | | 303K | 313K | 323K | (kJ/mol) | (J/mol) |
| FHLC | 7.07 | 11.93 | 12.17 | 12.46 | 8.52 | 63.57 |
| CGP | 7.07 | 11.68 | 11.98 | 12.15 | 7.67 | 67.42 |
| FHLC | 11.00 | 13.87 | 13.99 | 14.18 | 8.97 | 75.41 |
| CGP | 11.00 | 12.50 | 12.87 | 13.23 | 12.02 | 81.61 |

RSC Advances Accepted Manuscript